

Development Report:

Adaptation of a Small Robot for Paddy Fields to the Water Depth Change Using Variable Legs

Kentaro Kameyama and Takuya Wada

Division of Mechanical Engineering, National Institute of Technology, Fukui College

Geshi, Sabae, Fukui 916-8507, Japan

E-mail: k_kame@fukui-nct.ac.jp

[Received January 18, 2021; accepted August 24, 2021]

In this study, the authors conduct an operational test of a small weeding robot in paddy fields, and classify its behavioral incapacitations into two groups. Furthermore, the authors propose a leg structure for overcoming a sudden increase in water depth, one of the main causes of incapacitation. The robot is a two-wheeled vehicle with balance floats in the front and rear of the body, and the proposed structure enables the wheels to reach the ground by deforming the legs holding the wheels (variable-leg). The variable-leg robot is compared with a fixed-leg robot via a water tank experiment. It is verified that the variable-leg model can run at water depths of up to 180 mm, whereas the fixed-leg model can only run at water depths of approximately 80 mm. Furthermore, the variable-leg robot can adapt to dynamically changing water depths, as demonstrated by running over a hole.

Keywords: agricultural robot, traveling irregular ground, traveling mechanism

1. Introduction

Recently, the demand for organic agricultural products has been increasing, owing to the growing interest in food safety and environmental conservation. However, weeding has been a constraint to the implementation of products to satisfy such demand, as it requires a significant workforce. Furthermore, Japanese agriculture in general is currently facing a declining workforce. The use of robots is a promising approach to addressing these problems. In particular, the robotization of weeding work for rice crops is a critical issue owing to the large field areas, and several studies and developments have been conducted.

For example of agricultural robots based on existing farm machines, inter-row weeding robots made by adding weeding functions to rice transplanters have been proposed [1–4]. As examples of medium-sized weeding robots, robots for detecting ridges of seedlings with cameras and traveling via crawlers to destroy weeds have been proposed [5,6]. These robots are being tested for

their driving and weeding capabilities, and several challenges have been identified. One of the challenges is that these robots require an optimal ground bearing capacity in the field, because in weeding, the robot travels the same route several times, accordingly, the middle-sized robot can become incapacitated, owing to the soil type and its weight [7,8]. In addition, if the travel route is altered, the robot may destroy seedlings with its crawler and/or weight.

To address these challenges, the further downsizing of robots has been considered. To implement this concept, Seki et al. proposed a two-wheeled robot for detecting seedlings with contact sensors and weeding them with rotating brushes [9–11]. Furthermore, small robots can be used for surveys if the environment is not affected by the frequent entry of such robots in the field [12,13].

In contrast, small robots have the problem of being easily behaviorally incapacitated because they are easily affected by field conditions, such as the ground form and water depth. However, there are relatively few studies on the operation of small robots, and the problem is not well-defined. Therefore, one of the authors developed a prototype for a small weeding robot [14,15].

In this study, we conducted an operational test of the small weeding robot, and analyzed its behavioral incapacitation states. Accordingly, we proposed a moving mechanism for the robot that circumvents the water depth change, i.e., a main reason for the behavioral incapacitation. This paper is organized as follows. In Sections 2.1 and 2.2, we present the design concept of the small weeding robot and an overview of the operational test, respectively. In Section 2.3, we classify the states of the behavioral incapacitations occurring in the test and determine the improvement policy for the robot. Section 3 describes the design and prototyping of the moving mechanism, and an evaluation of the prototype using tank experiments is discussed in Section 4. Section 5 presents the conclusions of this study.



2. Design Strategy Based on Analysis of the Operational Test

2.1. Overview of the Small Robot for the Operational Test

In paddy fields, weed control using a robot can be achieved in two ways: (i) by shading effects owing to water muddiness, and (ii) by physical effects such as contact. For (i), a certain effect can be expected, regardless of the size and weight of the robot. In contrast, it is difficult to implement (ii) with a small robot, because the conventional method for controlling weeds physically is to use the robot to stamp weeds based on its crawlers and weight. Therefore, we adopted a chain-weeding method, as adopted in organic farming, for the test robot.

Chain weeding controls the sprouting of weeds in a shallow layer (upper layer higher than 20 mm) by bringing a chain into contact with weed seeds. Furthermore, it is assumed that weed seeds in the deep layer do not sprout. However, in the current implementation of chain weeding, a man or farm machine plows the soil heavily. In contrast, the small robot does not cause such a problem; hence, a chain-weeding method using a small robot is a promising practical implementation.

Hirose classified the mobility mechanisms of field robots into infinite rotation mechanisms such as wheels and crawlers, mobility by legs and body joints, or a combination of these mechanisms [16]. In this classification, crawler and body joint transfers are difficult to adopt from the perspective of being minimally invasive. Legs are also difficult to adopt, owing to their high surface pressure. Therefore, we adopted wheels for the moving mechanism of this robot; these were designed to reduce the surface pressure, similar to a rice planter.

Based on the above, a robot was built for the operational test. The overview and specifications of the test robot are presented in Fig. 1 and Table 1, respectively. The test robot was a radio-controlled two-wheeled vehicle equipped with balance floats in its front and rear. It was designed to work in paddy fields with a water depth of 50 mm. The width of the robot was within 300 mm (within the distance between the ridges). The maximum turning radius is approximately 207 mm. Although the float contacted seedlings during turning, the effect on the seedlings was assumed small, as there is sufficient space between the floats and ground.

The behavior of the robot is shown in Fig. 2. The robot was slightly tilted backward, and the gap between the body and the ground was approximately 30 mm.

The design value of the velocity was $V = 100$ mm/s. This value means that the test robot could weed a 1 a paddy field in 1 h, under the assumption that the travel distance in a paddy field with a 0.3 m furrow area was 333 m (1 a is a square area of 10×10 m). Then, the rotating speed of the geared motor could be expressed as follows:

$$R_m = \frac{V \times 60 \times d_g}{D \times \pi} = 327 \text{ rpm.} \quad \dots \dots \dots (1)$$

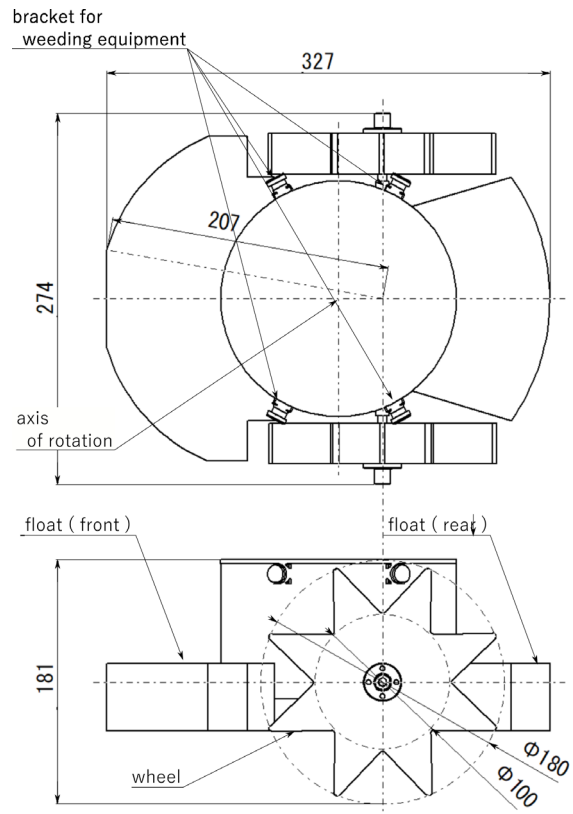


Fig. 1. Overview of the test robot for the operational test.

Table 1. Specification of the test robot.

Height × Width × Height [mm]		327 × 274 × 181
Weight (including battery) [kg]		1.8 (2.5)
Battery (rechargeable)	Voltage [V]	9.6 (1.2 × 8)
	Capacity [mAh]	7200 (2400 × 3)
Model No.: mfr.		380K75: TAMIYA Inc.
Geared motor	Rotating speed [rpm]	327
	Wattage [Wh]	8.6
Reduction gear ratio		20
Motor driver	Simple motor controller	
	Model No.: mfr.	18v7: pololu
	Max current [A]	14
Transceiver	Model No.: mrf.	RD8000/RX-831: SANWA

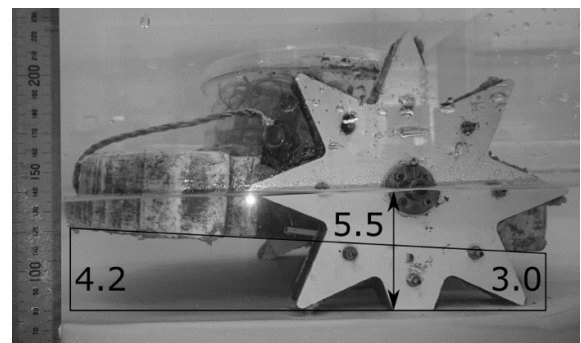


Fig. 2. Behavior of the test robot (water depth of 50 mm).

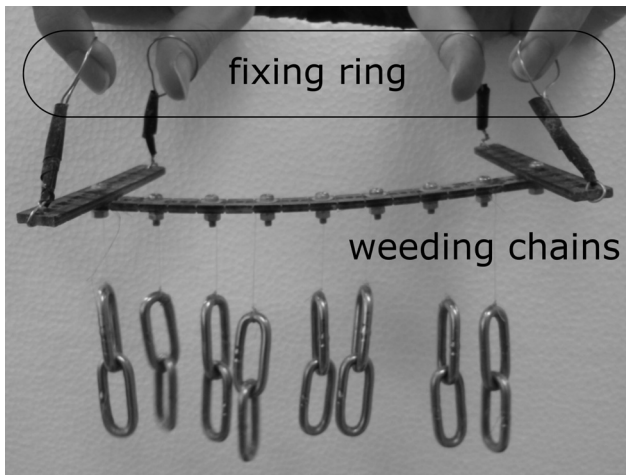


Fig. 3. Weeding unit.

In the above, it was assumed that the wheel radius is 114 mm, and $d_g = 20$ is the gear ratio of the intermediate gear.

Regarding the power supply, three units in which eight AA rechargeable batteries (1.2 V, 2400 mAh) are connected in series were adopted in parallel. Then, the expected battery life based on the power supply capacity and motor electricity consumption was $9.6 \times 7.2 / (8.6 \times 2) = 4.0$ h.

Figure 3 illustrates the weeding unit attached to the bottom of the robot. The length and weight of each chain were 90 mm and 50 g, respectively.

2.2. Outline of the Operational Test and Confirmation of the Traveling Ability

To validate the traveling ability and states of the behavioral incapacitations, an operational test using the test robot in a paddy field was conducted. Fig. 4 presents the appearance of the paddy field for the operational test, with 300 mm and 150 mm spacing between ridges and plants, respectively. The test was performed on the fore-boxed ridges. The test robot ran between the ridges in area A and over the ridges in area B to verify its traveling ability. The test started on May 11 (rice planting was done on May 9) and ended on June 4 (mid-drying). The dates and water depths are presented in Table 2. No driving tests were conducted on days marked with “-” in the calendar. The water depths were measured using a fixed ruler.

Prior to the operational test, we verified the traveling ability (velocity and battery life) in an expected environment (water depth of 50 mm, with no extreme rises or deformations in the ground) in an open area of the paddy.

At the beginning of the test, the robot achieved a design velocity of $V = 100$ mm/s. In addition, the test robot was not incapacitated during this test. However, the battery life was 0.5 h, and the traveling distance was 150 m if we assumed that the experiment ended when the robot’s speed decreased to half of its initial speed. This result meant that two robots could weed a 1 a paddy field in 0.5 h.

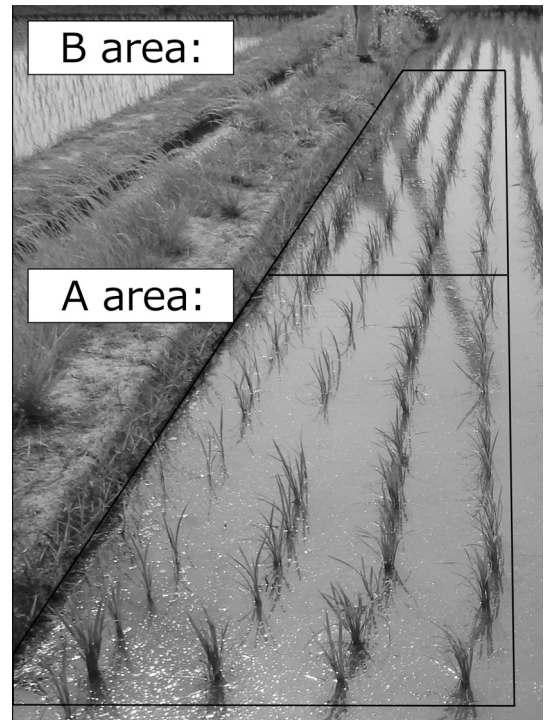


Fig. 4. Paddy field for the operational test and its partitioning.

Table 2. Test dates and water depth.

Sun.	Mon.	Tue.	Wed.	Thu.	Fri.	Sat.
10	11	12	13	14	15	16
-	50	-	50	70	70	-
17	18	19	20	21	22	23
-	70	80	-	50	80	-
24	25	26	27	28	29	30
-	60	50	50	-	-	-
31	1	2	3	4	5	6
-	50	30	-	30	-	-

[mm]

2.3. Design Strategy Based on the Classification of the Behavioral Incapacitations

The behavioral incapacitations states were classified into three cases. The classified cases and examples are presented in Figs. 5 and 6–8, respectively.

Case 1 involves the disruptions caused by shallow water, and Case 1-1 represents the stranding case, i.e., when the robot rises up on the ridges. Fig. 6 illustrates the stranding case occurring when the robot ran across the ridge in area B. A similar case (Case 1-2, Fig. 7) is the stranding case when the robot rides on an underwater obstacle, such as a rice stump. This case occurred when the robot ran between ridges. This also occurred when the water depth was 30 mm or less, because the pitch motion around the wheel axle was limited so far as avoiding

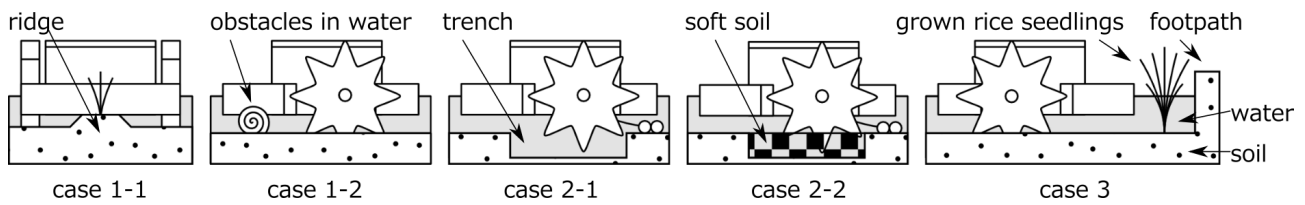


Fig. 5. Classified states of the behavioral incapacitations: (Case 1-1) riding on a ridge, (Case 1-2) riding on an underwater obstacle or ashore, (Case 2-1) decrease in the driving force caused by the depth, (Case 2-2) decrease in the driving force triggered by the soft soil, (Case 3) collision against ridges or grown seedlings.

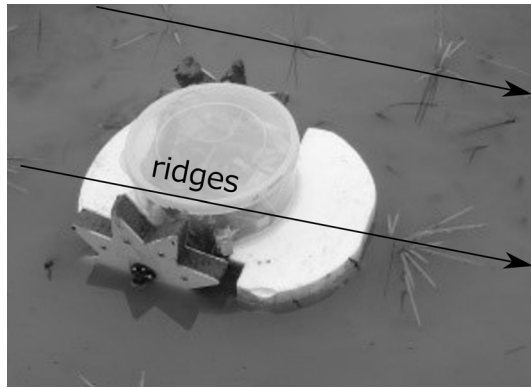


Fig. 6. Example of the accident in Case 1-1 (stranding owing to ridge bulge).



Fig. 7. Example of the accident in Case 1-2 (left) and the causal obstacle (right).



Fig. 8. Example of the accident in Case 3 (collision on seedlings).

Table 3. Classified states of the behavioral incapacitations.

Case	1-1	1-2	2-1	2-2	3
State of behavioral incapacitation	Stranding		Decrease of driving force		Collision
Cause	Ridge	Obstacle in water	Trench	Soft soil	Seedling, ridge
Signature	○	○	×	○	×
Possibility to return	×	×	×	×	○
Group	1	1	2	1	1

obstacles. In these cases, it was difficult to avoid obstacles by sight because they existed under the water surface. However, the robot did not become incapacitated immediately after contacting such obstacles. Before the robot becomes incapacitated, signatures could be observed, such as loss of mobility or control performance; in general, a robot becomes incapacitated not by collisions, but by riding up (the increase in the contact area between the robot’s body and the ground). Case 2 is the state of behavioral incapacitation owing to a decrease in thrust force triggered by increased water depth, footprints, and the wheel tracks of farm machines (Case 2-1), or soft soil (Case 2-2). Similar signatures to those in Cases 1 and 2-2 were expected when going up and down a slope, respectively. In these cases, we could not identify the obstacles by sight.

Collisions with rice seedlings and the boundaries of paddy fields were classified as Case 3. **Fig. 8** presents an illustration of a collision with rice seedlings. Three weeks after transplanting, it became difficult for the robot to overcome the rice seedlings. In Case 3, the robot becomes incapacitated if it runs until it rides up on a seedling. However, the robot could return to its ordinary state by detecting collisions in the early stages.

Ultimately, these examples were classified from the perspectives of the behavioral incapacitation states, causes, presence or absence of the signatures, and possibility of recovery (**Table 3**). Furthermore, we classified Cases 1 and 2-2, which are unrecoverable but have signatures, as Group 1. Similarly, Case 2-1, which is unrecoverable and has no signatures, was classified as Group 2. Case 3, which is recoverable after a collision, was classified as Group 1.

Based on the above, we considered a design proposal comprising two detailed plans for addressing the problems of incapacitation. For Group 1, the robot detected the signature using an accelerometer, and avoided behav-

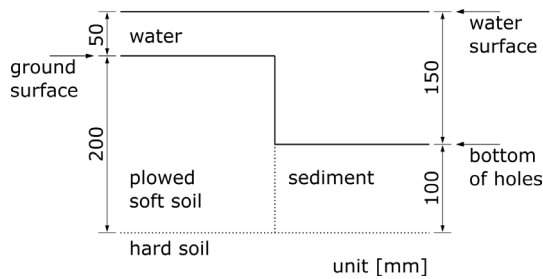


Fig. 9. Depth of paddy fields.



Fig. 10. Experimental robot (left) and its traveling test in the water tank (right).

ioral incapacitation. For Group 2, we modified the structure of the robot such that it did not become incapacitated, even if the water depth increased abruptly. In this paper, a method for addressing the latter problem is discussed.

3. Design and Fabrication of the Variable-Leg for the Robot

Figure 9 presents the basic concept of water depth in paddy fields. In a typical paddy field, the depths of the holes created by footprints and wheel tracks of farm machines are up to 200 mm below the ground surface, because the soil is plowed to a depth of 150–200 mm. Furthermore, with time, the holes are covered with the surrounding soil, and the depth of the holes will become approximately 50–100 mm. Consequently, assuming that the water depth from the ground surface is 50 mm, the maximum depth that the robot must travel is 150 mm.

According to the above requirements, the amount of water depth fluctuation that the robot must respond to was verified by water tank experiments using an experimental robot. The experimental robot had dimensions of 240 mm × 365 mm × 240 mm and a weight of 3.3 kg and is illustrated in **Fig. 10**. It was built based on the same concept as the test robot, and its posture in water was the same as that of the test robot (**Fig. 11**).

The dimensions of the tank were 1800 mm × 900 mm × 900 mm. To visualize the behavior of the robot, we adopted a 1 : 1 : 2 mixture of three types of glass beads with particle sizes of 1.0–0.71 mm, 0.5–0.355 mm, and 0.053–0.038 mm (FGB-20, 40, 320, Fuji Glass Beads Inc.). The mixture ratio was determined by a simple evaluation of the flat plate sinking behavior characteristics, such that the mechanical properties of the paddy soil

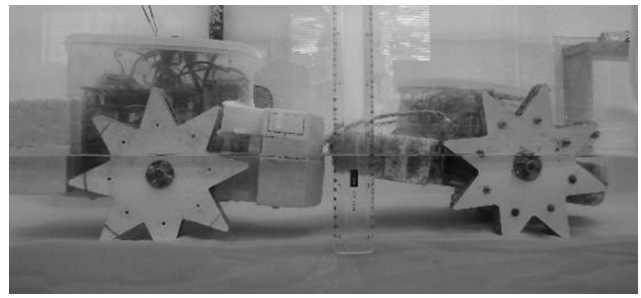


Fig. 11. Comparison of the postures of the experimental robot (left) and the test robot (right).

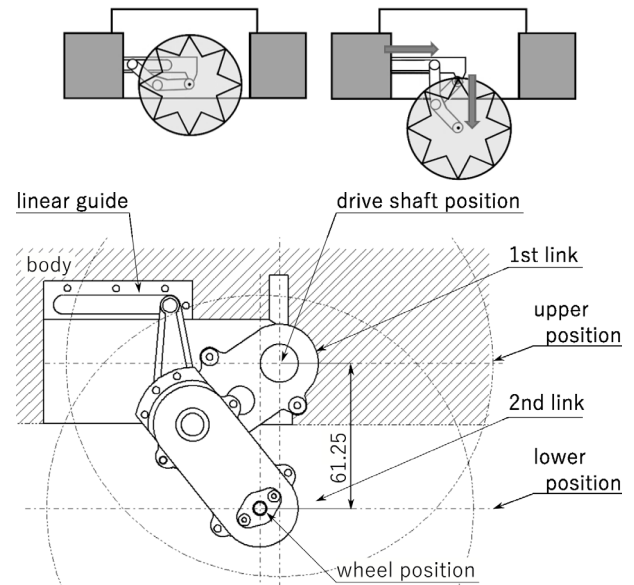


Fig. 12. Concept illustration of the variable-leg.

and glass bead mixture were similar [17] (for the design details, see Appendix A). The sediment thickness was 50 mm.

In this water tank, the experimental robot could move forward, backward, and turn at a maximum depth of 90 mm; hence, the robot need to travel at an additional water depth of 60 mm.

To achieve this goal, there are several ways to introduce auxiliary propulsion (e.g., screw) or to make the wheels reach the ground. In the experimental robot, we decided to adopt the latter method, because the experimental robot was utilized for task that required traction force, such as chain weeding. Specifically, we adopted a method in which the wheels reached the ground by deforming the legs supporting the wheels.

Figure 12 presents a conceptual illustration of the variable leg. This leg comprises two links, i.e., the first (body side) and the second (wheel side) links. Each link contains three gears and can transmit the driving power. There is no power available to raise or lower the wheel; hence, the wheel reaches the ground according to gravity. The trajectory of the wheels is constrained vertically downward from the drive shaft position, as the second link is

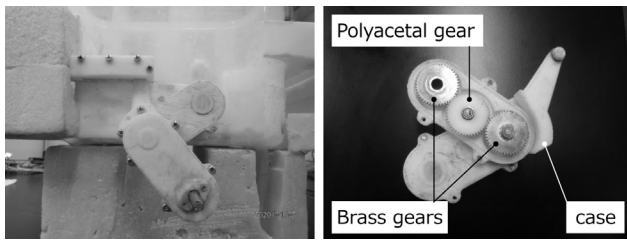


Fig. 13. Experimental robot with variable-leg (left) and inner structure of the variable leg (right).

Table 4. Results of the traveling test.

Water depth [mm]	Fixed-leg	Variable-leg
190–200	Adrift	Adrift
180	Adrift	Unstable
100–170	Adrift	Stable
90	Unstable	Stable
80	Stable	Stable
70	Stable	Gear trouble
10–60	Stable	Gear trouble

constrained to the horizontal slide rail on the body using the rod.

Figure 13 illustrates the experimental robot with variable legs. The cases were printed using an FDM-type 3D printer (M200, Zortrax) with ABS-like mixed material (z-ultra basic, Zortrax). A polyacetal gear (center) and two brass gears (both sides) were included in each case. The maximum wheel droop distance in this prototype was approximately 65 mm, meeting the 60 mm requirement.

The weights of the upper link (W_u), lower link (W_l), and wheels (W_w) of the prototype variable leg were 77 g, 79 g, and 138 g, respectively, and the buoyancy forces F_u , F_l , and F_w were 36 g, 36 g, and 122 g, respectively. In this implementation, the legs were designed to be lightweight, so as to reduce the load on the drive system and structure. If the speed of the robot was high and a quick response of the wheel was required, the weight of the wheels could be increased or static actuators (such as springs) could be used to drive the legs.

4. Evaluation of the Experimental Robot’s Traveling Ability in the Water Tank

The adaptive capability of the experimental robot with the variable leg (variable-leg model) to changes in water depth was tested via a water tank experiment. The experimental description is the same as that for the experimental robot with a fixed leg (fixed-leg model). The results for both models are presented in **Table 4**, and the wheel positions of the variable-leg model at water depths of 180, 170, 70, and 60 mm are presented in **Fig. 14**. As

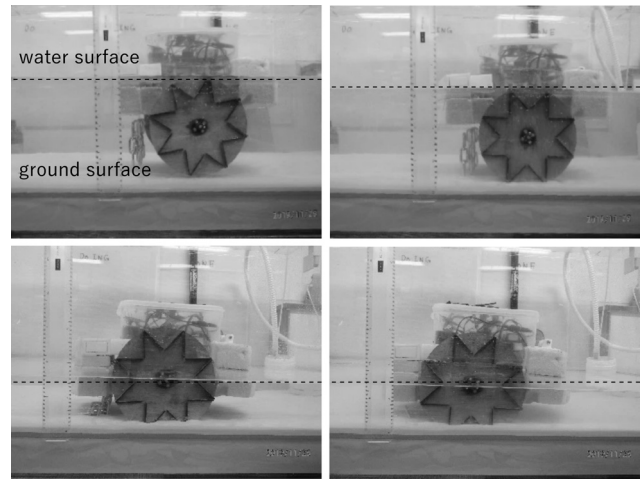


Fig. 14. Traveling test of the robot in the water tank in the cases with water depths of 180 mm (upper left), 170 mm (upper right), 70 mm (lower left), and 60 mm (lower right).

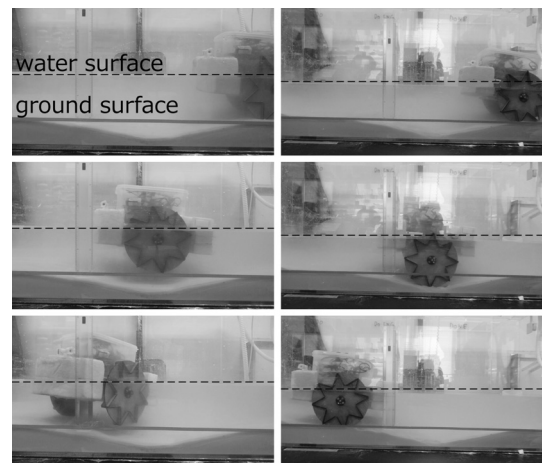


Fig. 15. Video illustrations of the traveling test for the fixed-leg (left column) and variable-leg (right column) models.

shown, the fixed-leg model can run within a water depth of 80 mm, whereas the variable-leg model can run at a water depth of 180 mm. In contrast, for the variable-leg model, the problem of slipping the internal gears occurs when turning and moving forward and moving backward rapidly at a water depth of 70 mm. Furthermore, the polyacetal gear is damaged at a water depth of 60 mm.

Finally, the following capability of the wheel was tested when the water depth changed dynamically. In this experiment, the water depth was 80 mm, and the hole width and maximum hole depth were 400 mm and 50 mm, respectively. The robot speed was 100 mm/s. **Fig. 15** presents a few video frames. The left side of **Fig. 15** shows that the fixed-leg model cannot travel, because its wheel leaves the ground. In contrast, the right figure shows that the wheels of the variable-leg model follow the ground and proceed over the hole.

From the above, although the stiffness design needs to be considered, it can be inferred that the variable-leg

model can run at a water depth of 180 mm and can follow dynamic changes in water depth.

5. Conclusions

In this study, we proposed a small robot for paddy fields with a mechanism that changes the relative position of its wheels and body to avoid the incapacitation of the robot in deep water. The target robot is a vehicle-type robot that runs on two wheels in paddy fields with a water depth of 50 mm, and the proposed mechanism enables the robot to run in paddy fields with water depths of up to 180 mm.

To achieve the above objective, we first conducted an operational test in a paddy field and classified the states of the behavioral incapacitations into two groups, based on the existence of incapacitation signatures and possibility of recovery. In this study, we attempted to address the problem of a sudden increase in water depth, i.e., one that cannot be recovered from or detected beforehand (Group 2).

To address this problem, we proposed a mechanical method to enable the wheels to reach the ground by deforming the legs supporting the wheels.

The experimental robot was tested in a water tank, and we found that the fixed-leg and variable-leg models could run at water depths of 80 mm and 180 mm, respectively. We also verified that the wheels of the variable-leg model could follow the ground even if the water depth changed dynamically. Based on these results, we validated the effectiveness of the proposed method.

A future direction will be to address the gear slipping problem at shallow water depths, as triggered by the increased complexity and weight of the robot. We believe that this problem can be addressed by appropriately designing the force specifications (chain traction, thrust, buoyancy, etc.) and structure during the study process of implementing variable legs on any robot.

Furthermore, for the comfortable driving of small paddy field robots, a solution for Group 1 cases (the cases involving robot recovery by detecting the signature of collision) is required; in particular, a collision detection method for soft deformable objects, such as mud, and a corresponding avoidance algorithm, are required. In addition, the optimal migratory pathways in paddy fields may differ from those on land because small robots are easily affected by field conditions. Therefore, it is necessary to develop efficient guidance methods for both local and entire field conditions.

References:

- [1] M. Saito, Y. Nagasaka, K. Tamaki, and K. Kobayashi, "Paddy Weeding Using an Autonomous Rice Transplanting Robot: Evaluation of Traveling Accuracy and Effect on Seedlings," *J. of the Japanese Society of Agricultural Machinery*, Vol.72, pp. 276-282, 2010 (in Japanese).
- [2] Y. Miyahara, K. Tosaki, T. Ichikawa, F. Kuroiwa, and M. Orimoto, "Development of a High-Precision Weeder for Paddy Fields (1st Report)," *J. of the Japanese Society of Agricultural Machinery*, Vol.63, pp. 37-38, 2001 (in Japanese).
- [3] Y. Miyahara, T. Kanuma, T. Ichikawa, M. Matsuoka, and M. Orimoto, "Development of a High-Precision Weeder for Paddy Fields (2nd Report)," *J. of the Japanese Society of Agricultural Machinery*, Vol.64, pp. 47-48, 2002 (in Japanese).
- [4] M. Orimoto, M. Matsuoka, Y. Miyahara, T. Kanuma, and T. Ichikawa, "Development of a High-Precision Weeder for Paddy Fields (3rd Report)," *J. of the Japanese Society of Agricultural Machinery*, Vol.65, pp. 77-78, 2003 (in Japanese).
- [5] H. Sori, H. Inoue, H. Hatta, and Y. Ando, "Effect for a Paddy Weeding Robot in Wet Rice Culture," *J. Robot. Mechatron.*, Vol.30, No.2, pp. 198-205, 2018.
- [6] K. Fujii, K. Tabata, T. Yokoyama, S. Kudomi, and Y. Endo, "Development of a Small Weeding Robot "AIGAMO ROBOT" for Paddy Fields (7th Report)," *Gifu Prefectural Industrial Technology Center Research Report*, Vol.17, pp. 48-51, 2015 (in Japanese).
- [7] R. Kawaguchi, "Paddy Weed Machine," *Japanese Society of Agricultural Machinery and Food Engineers*, Vol.80, pp. 356-360, 2018 (in Japanese).
- [8] K. Fujii, K. Tabata, T. Yokoyama, H. Hirayu, and Y. Endo, "Development of a Small Weeding Robot "AIGAMO ROBOT" for Paddy Fields (5th Report)," *Gifu Prefectural Industrial Technology Center Research Report*, Vol.15, pp. 32-34, 2013 (in Japanese).
- [9] M. Seki, H. Nishida, and K. Takahashi, "Development of an Environment-Harmonized Weeding Robot System (1st Report)," *J. of the Japanese Society of Agricultural Machinery*, Vol.60, pp. 109-110, 1998 (in Japanese).
- [10] M. Seki, H. Nishida, K. Takahashi, and K. Kojima, "Development of an Environment-Harmonized Weeding Robot System (2nd Report)," *J. of the Japanese Society of Agricultural Machinery*, Vol.61, pp. 277-278, 1999 (in Japanese).
- [11] M. Seki, H. Nishida, K. Takahashi, and K. Kojima, "Development of an Environment-Harmonized Weeding Robot System (3rd Report)," *J. of the Japanese Society of Agricultural Machinery*, Vol.62, pp. 51-52, 2000 (in Japanese).
- [12] K. Kameyama, Y. Kakitani, S. Kimura, and K. Murashima, "Development of the Soil Sampler for the Small Moving Robot," *The Robotics and Mechatronics Conf. 2017 (ROBOMECH2017)*, 1A1-B01, 2017 (in Japanese).
- [13] K. Kameyama, K. Sasaki, and M. S. B. Basir, "Development of the Chemical Ingredients Sensing Robot for the Paddy Fields," *The Robotics and Mechatronics Conf. 2018 (ROBOMECH2018)*, 1A1-A02, 2018 (in Japanese).
- [14] K. Kameyama, T. Yasuoka, R. Kawakami, and N. Asai, "Development of the Robot to Inhibit Growth of Weeds in the Paddy Field," *The Proc. of the JSME Annual Meeting*, G150031, 2012 (in Japanese).
- [15] K. Kameyama, Y. Yamada, and D. Kado, "Development of a Less Invasive Small Robot for Paddy Fields," *Joint Conf. on Environmental Engineering in Agriculture 2018*, PA-21, 2018 (in Japanese).
- [16] S. Hirose, "Mechanical Design of Mobile Robot for External Environments," *J. of the Robotics Society of Japan*, Vol.18, pp. 904-908, 2000 (in Japanese).
- [17] Committee for Tire Design Guidelines, the Japanese Society for Terramechanics, "Terramechanics Library 1: Off-road Tire Engineering – Fundamentals of Design and Performance Prediction –," *Proc. of the Japanese Society for Terramechanics*, Kyoto, 1999 (in Japanese).

Appendix A. Evaluation of Mechanical Properties of Soil via the Flat Plate Sinking Behavior Characteristics

The performance of a wheel traveling over a rough terrain or soft soil depends on both the performance of the wheel and the mechanical properties of the soil. The mechanical properties of soil are influenced by the shape, size, and moisture content of the particles. The particle sizes of the soil constituents are listed in **Table 5** [17]. In this study, the mixture ratio of glass beads was determined by evaluating flat-plate sinking behavior characteristics; this is a method for measuring and expressing the mechanical properties of soil and is often used for evaluating soft ground.

Table 5. Particle sizes of soil constituents.

	Size [mm]
Gravel particle	≥ 2.0
Coarse sand	2.0–0.42
Fine sand	0.42–0.075
Silt	0.075–0.005
Cray	≤ 0.005

Table 6. Mixture ratios of glass beads for bottom material.

	FGB-20	FGB-40	FGB-320
A	1	1	1
B	1	1	2
C	1	1	2.5

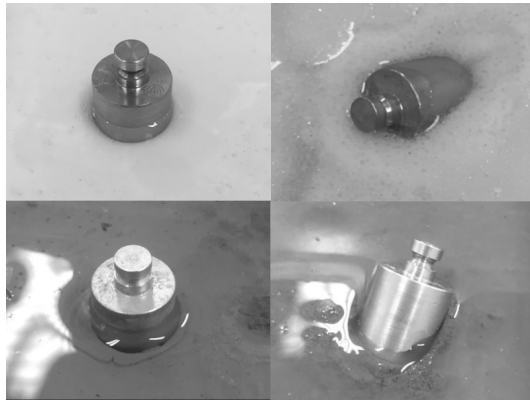


Fig. 16. Illustration of the behaviors of the weights in the evaluation (upper: glass beads, lower: soil / left: upright, right: overturned).

Table 7. Results of the evaluation of flat plate sinking behavior characteristics (○: upright, ×: overturned).

	A	B	C	Soil
10 g	○	○	○	○
20 g	×	○	○	○
50 g	×	×	○	×

This method elucidates the properties of soil by penetrating a plate into the soil and measuring the relationship between the penetration depth and resistance. In this evaluation, the authors performed a simple evaluation by comparing the behaviors of different flat weights penetrating the soil.

The evaluation was conducted by placing 10 g, 20 g, and 50 g weights on the surface of the three-glass bead mixtures presented in **Table 6** and paddy soil, and comparing their behaviors. The experiment and results are shown in **Fig. 16** and **Table 7**, respectively. The behav-

iors of the weights placed on the soil surface were classified into two groups: those that remained upright, and those that overturned after sinking. The obtained results indicate that increasing the ratio of fine beads improves the load-holding capacity.

Based on the above, mixture ratio B was adopted under the assumption that the mixture ratio with a similar behavior would also have a similar ability to receive force from the wheels.



Name:
Kentaro Kameyama

Affiliation:
Department of Mechanical Engineering, National Institute of Technology, Fukui College

Address:
Geshi, Sabae, Fukui 916-8507, Japan

Brief Biographical History:
2006- Lecturer, National Institute of Technology, Fukui College
2009- Associate Professor, National Institute of Technology, Fukui College

Main Works:
• “Subspace-based Prediction of Linear Time-varying Stochastic Systems,” *Automatica*, Vol.43, No.12, pp. 2009-2021, 2007.

Membership in Academic Societies:
• The Japan Society of Mechanical Engineering (JSME)
• The Society of Instrument and Control Engineers (SICE)
• The Institute of Systems, Control and Information Engineers (ISCIE)
• The Japanese Society of Agricultural Machinery and Food Engineers (JSAM)



Name:
Takuya Wada

Affiliation:
Department of Mechanical Engineering, National Institute of Technology, Fukui College

Address:
Geshi, Sabae, Fukui 916-8507, Japan

Brief Biographical History:
2019- Kanazu Mill, Rengo Co., Ltd.

Main Works:
• Agricultural robot